Resummation of the α expansion for nonlinear pair production by an electron in a strong electromagnetic field

Greger Torgrimsson*

Department of Physics, Umeå University, SE-901 87 Umeå, Sweden

(Received 25 July 2022; accepted 4 January 2023; published 30 January 2023)

We show how to resum the Furry-picture α expansion in order to take quantum radiation reaction and spin transition into account in the nonlinear trident process in (pulsed) plane-wave background fields. The results are therefore nontrivial functions of both the background field strength, eE, and the coupling to the quantized photon field, $\alpha = e^2/4\pi$. The effective expansion parameter, T, is α times $eE/m\omega \gg 1$, which makes higher orders in α important. We show that they can change the sign of the spin-dependent part already at $T < 1$, which will be experimentally accessible. We also present a new resummation method that essentially does to a convergent series what Borel-Padé resummation does to an asymptotic series.

DOI: 10.1103/PhysRevD.107.016019

I. INTRODUCTION

The nonlinear trident process [1–14] in a strong electromagnetic background field (e.g., from a laser), $e^- \to e^-e^-e^+$, is an experimentally important process in strong-field QED; see Refs. [15–17] for reviews. It was measured in an experiment [1] that was the first and, for a long time, basically the only experiment in this research field. Back then, the lasers were actually relatively weak, i.e., $a_0 = E/\omega < 1$.[1] Laser intensities have since increased steadily, and it is now possible to have $a_0 \gg 1$. There are plans to measure trident again but now in a genuinely strong-field regime, e.g., by LUXE [18] or FACET-II [19].

For $a_0 > 1$, one cannot treat the background field in perturbation theory. The quantized photon field, though, is still treated in perturbation theory, which gives $P_{\text{trident}} = \alpha^2 F(E)$ to leading order in $\alpha = e^2/4\pi$, where F is some nontrivial function. This $\mathcal{O}(\alpha^2)$ has been studied in several recent papers [4–14], and we now have a much better understanding of how to calculate it.

However, for $a_0 \gg 1$, the effective expansion parameter is $T = a_0\alpha$, which is not small, i.e., $\mathcal{O}(\alpha^2)$ may not be enough. In this paper, we present methods for how to resum all orders in α and show that this is important even for $T \lesssim 1$.

Various resummations of the α expansion appear in several recent papers on radiation reaction (RR) [20–24] and other processes [25–31]. Comparing with the resummations in Refs. [25,26] or [27,28], we see that we all consider "strong-field" regimes where the dominant contribution comes from some sort of reducible diagrams. However, these are nevertheless very different regimes and resummations. References [27,28] resummed loop diagrams for $\alpha\chi^{2/3} \gtrsim 1$, i.e., $\chi \gg 1$, in order to study the Ritus-Narozhny conjecture [32,33], while we consider $\chi \lesssim 1$. References [25,26] considered a very different regime where the dominant contribution comes from tadpole loop diagrams, which were believed to vanish until Ref. [34]. The fields we consider are much weaker and can be approximated as plane waves, and tadpoles have been shown to vanish for plane waves [35,36]. Another difference is that, for the quantities and regimes we consider, we need to resum both sums over loops as well as sums over the number of final-state particles.

II. DERIVATION

Figure 1 illustrates which processes are included and which ones are neglected. The particular diagram in Fig. 1 represents one typical process. We are interested in the infinite sum of the probabilities to produce one pair together with $0, 1, 2, 3\ldots$ photons. The amplitude to produce one pair and n photons is itself given by an infinite coherent sum of $0, 1, 2, 3\ldots$ loops. These one-particle reducible loops give the dominant contribution for large a_0 or a long pulse [30,31,37,38]. We showed in Refs. [38,39] how to write the dominant contribution of $\mathcal{O}(\alpha^n)$ processes with products of $\mathcal{O}(\alpha)$ "strong-field-QED Mueller matrices" (**M**), which describe how the fermion spin/photon polarization Stokes vectors (**N**) change. This is

*greger.torgrimsson@umu.se

[1]We absorb e into the laser field strength, $eE \to E$, and use units with $c = \hbar = m_e = 1$.

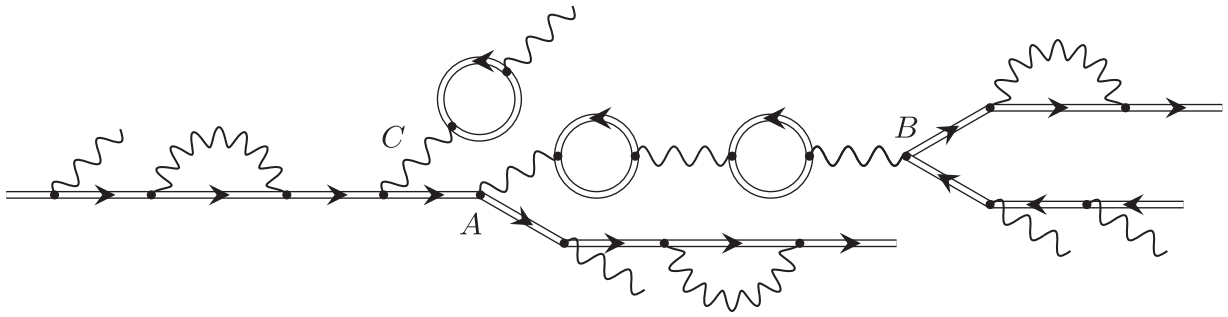

FIG. 1. Typical diagram for trident at higher orders.

similar to how ordinary Mueller matrices work in optics, where the Stokes vector of a light beam changes to $\mathbf{N} \to \mathbf{M} \cdot \mathbf{N}$, after passing through an optical element characterized by $\mathbf{M}$. In our case, the $\mathbf{M}$'s are not constant but depend on (light-front) time and the momentum. An important point is that both real particle production and loops can be treated using sums of incoherent products of Mueller matrices, so we have, e.g., one Mueller matrix, $\mathbf{M}^C$, for photon emission and one for the fermion-mass loop, $\mathbf{M}^L$. We showed in Refs. [21,22] how to evaluate and resum the resulting α expansion for the case with no pair production. Here, we take the next step and consider the production of one pair. We therefore neglect terms and processes that are more exponentially suppressed than the leading exponential scaling, which is $\exp(-16/[3\chi])$ for a constant field, where $\chi = \sqrt{-(F^{\mu\nu}p_\nu)^2}$ is the quantum nonlinearity parameter for a particle with momentum p_μ, which gives the field strength as seen in the rest frame.

Consider first the photon emissions and loops on the electron line after vertex A in Fig. 1 and on the fermion line connected to vertex B. When we resum these diagrams, we find sums of (schematically) $\int(\mathbf{M}^C + \mathbf{M}^L) \cdot (\mathbf{M}^C + \mathbf{M}^L) \cdot \ldots \cdot (\mathbf{M}^C + \mathbf{M}^L)$. We will come back to the details below, when we consider a similar resummation for the line before vertex A. At this point, it is enough to note that if we sum over the spins of the final-state particles, then we should multiply this with the Stokes vector that describes unpolarized particles, i.e., $\mathbf{N} = \{1, \mathbf{0}\}$, but we have $(\mathbf{M}^C + \mathbf{M}^L) \cdot \{1, \mathbf{0}\} = \{0, \mathbf{0}\}$, so the resummation of these terms collapses, and we find that we do not actually need to consider the photon emissions and loops on these final-state lines.

The sum over all fermion loops[2] between vertex A and B can be expressed in compact form as Eq. (147) in Ref. [38]. We find that one part of this sum can be neglected as long as production of more than one pair is negligible. The other part describes how the photon $\mathbf{N}_\gamma$ rotates between A and B. This vacuum birefringence part does not contribute here since we consider initial- and final-state fermions that are either unpolarized or polarized parallel (or antiparallel) to the magnetic field of the linearly polarized background, and in this case, the components of $\mathbf{N}_\gamma$ that would rotate drop out. The sum of the fermion loops on externally emitted photons, e.g., the photon line starting at C, can again be neglected as long as multiple pair production is negligible. We thus find that what we need to consider is the sum over all photon emissions and loops attached to the electron line up to vertex C.

Note that, as this is a first-principles approach, there is no need to "add" a quantum Landau-Lifshitz equation, the T-BMT equation for spin precession or the Sokolov-Ternov effect; those effects are already automatically included in the resummation of $\mathbf{M}^C$ and $\mathbf{M}^L$ [21,22].

We consider plane-wave backgrounds, which is motivated by the fact that a high-energy electron sees a rather general field as if it were a plane wave. Plane waves only depend on light-front time, $\sigma = kx = \omega(t+z)$ (k_μ is the wave vector of the field), so the other coordinates give trivial integrals. And only the longitudinal[3] momentum component, $kp/2\omega = p'_- = (p'_0 - p'_3)/2 > 0$, plays a nontrivial role, as the perpendicular integrals factorize and can therefore be performed for each Mueller matrix separately, which has already been done.

To obtain $\mathcal{O}(\alpha^n)$, we start with the latest vertex, i.e., B in Fig. 1, and work backward in time. Since we sum over the final-state spins, in this step, we only need a Mueller vector rather than matrix, which takes into account the dependence on the polarization of the intermediate photon. Here, we use[4] $s_2 = kp_2/kl$ and $s_3 = kp_3/kl = 1 - s_2$ for the ratios of the longitudinal momenta of the electron (momentum p_2^μ) and positron (p_3^μ), respectively, and the photon (l^μ). At each step, we let $b_0 = kp'$, where p'_μ is the momentum of whatever particle that goes into that step, so in this step, $b_0 = kl$. The Mueller vector we need is given by [38]

[2]See also Refs. [37,40,41] for different formulations of all-order birefringence [40,41] or quantities that correspond to sums over loops.

[3]Since p'_3 never appears separately in this paper, we drop "light front" and simply call p'_- the longitudinal momentum.

[4]Lorentz contractions are denoted simply $kp = k_0 p_0 - k_j p_j$.

$$\mathbf{M}^{BW}(\chi, s_3) = \begin{pmatrix} \mathrm{Ai}_1(\xi) - \kappa\frac{\mathrm{Ai}'(\xi)}{\xi} & \frac{\mathrm{Ai}'(\xi)}{\xi} \end{pmatrix}, \quad (1)$$

where $\mathrm{Ai}_1(\xi) = \int_\xi^\infty \mathrm{d}x\,\mathrm{Ai}(x)$, and[5] $\xi = (r/\chi)^{2/3}$, $r = (1/s_2) + (1/s_3)$, $\kappa = (s_2/s_3) + (s_3/s_2)$, and $\chi = \chi_0|f'(\sigma)| = a_0 b_0 |f'(\sigma)|$ is the locally constant value of $\chi = \sqrt{-(F^{\mu\nu}l_\nu)^2}$ for a field with potential $a_\mu(\sigma) = \delta_{\mu 1} a_0 f(\sigma)$. We construct a σ-dependent Stokes vector,

$$\mathbf{N}^{(1)}(\chi_0, \sigma) \coloneqq \int_\sigma^\infty \frac{\mathrm{d}\sigma'}{\chi_0} \int_0^1 \mathrm{d}s_3 \mathbf{M}^{BW}(\chi, s_3). \quad (2)$$

The lower integration limit, σ, allows us to prepend the earlier Mueller matrices with time ordering. An initial-state photon with Stokes vector $\mathbf{N}$ would, to leading order in α, decay into a pair with probability $P = \mathbf{N}_\gamma \cdot \mathbf{N}^{(1)}(\chi_0, -\infty)$. In general, Stokes vectors have four elements, but for the cases we consider here, only two of them are relevant. $\mathbf{N}_\gamma = \{1, \pm 1\}$ and $\mathbf{N}_\gamma = \{1, 0\}$ correspond to photon polarization parallel to the electric and magnetic fields and to an unpolarized photon.

The next step is vertex A, which has the structure $\mathbf{N}_0 \cdot \mathbf{M}^C_{0\gamma} \cdot \mathbf{N}_\gamma$ where $\mathbf{N}_0$ is the Stokes vector for the electron before emitting the photon. $\mathbf{N}_0$ too is reduced from a vector with four to two elements, where $\mathbf{N}_0 = \{1, \pm 1\}$ and $\mathbf{N}_0 = \{1, 0\}$ correspond to spin (anti)parallel to the magnetic field and to an unpolarized state. The momentum of the electron before and after emitting the photon is p_μ and $p_{1\mu}$, respectively, so for this step, we let $b_0 = kp$. We also use $q = kl/kp$ and $s_1 = kp_1/kp = 1 - q$. The effectively 2×2 Mueller matrix is given by

$$\mathbf{M}^C_{0\gamma}(\chi, q) = \begin{pmatrix} -\mathrm{Ai}_1(\xi) - \kappa\frac{\mathrm{Ai}'(\xi)}{\xi} & -\frac{\mathrm{Ai}'(\xi)}{\xi} \\ q\frac{\mathrm{Ai}(\xi)}{\sqrt{\xi}} & \frac{q}{s_1}\frac{\mathrm{Ai}(\xi)}{\sqrt{\xi}} \end{pmatrix}, \quad (3)$$

where now $\xi = (r/\chi)^{2/3}$, $r = (1/s_1) - 1$ and $\kappa = (1/s_1) + s_1$. We again define a σ-dependent Stokes vector,

$$\mathbf{N}^{(2)}(\chi_0, \sigma) = \int_\sigma^\infty \frac{\mathrm{d}\sigma'}{\chi_0} \int_0^1 \mathrm{d}q\, \mathbf{M}^C_{0\gamma}(\chi, q) \cdot \mathbf{N}^{(1)}(q\chi_0, \sigma'). \quad (4)$$

Note that we now have $q\chi_0$ instead of χ_0 in the argument of $\mathbf{N}^{(1)}$ since at each step we use b_0 for the momentum of whatever particle that is present just before that step.

Starting from $\mathbf{N}^{(3)}$, we have the same recursive formula as in Refs. [21,22]. For an electron experiencing RR, we need two Mueller matrices, one for Compton scatting

$$\mathbf{M}^C(\chi, q) = \begin{pmatrix} -\mathrm{Ai}_1(\xi) - \kappa\frac{\mathrm{Ai}'(\xi)}{\xi} & \frac{q}{s_1}\frac{\mathrm{Ai}(\xi)}{\sqrt{\xi}} \\ q\frac{\mathrm{Ai}(\xi)}{\sqrt{\xi}} & -\mathrm{Ai}_1(\xi) - 2\frac{\mathrm{Ai}'(\xi)}{\xi} \end{pmatrix} \quad (5)$$

and one for the fermion-mass loop (see Fig. 1)

$$\mathbf{M}^L(\chi, q) = \begin{pmatrix} \mathrm{Ai}_1(\xi) + \kappa\frac{\mathrm{Ai}'(\xi)}{\xi} & -q\frac{\mathrm{Ai}(\xi)}{\sqrt{\xi}} \\ -q\frac{\mathrm{Ai}(\xi)}{\sqrt{\xi}} & \mathrm{Ai}_1(\xi) + \kappa\frac{\mathrm{Ai}'(\xi)}{\xi} \end{pmatrix}, \quad (6)$$

with the same ξ and κ as for $\mathbf{M}^C_{0\gamma}$. (Here, we can explicitly see that $(\mathbf{M}^C + \mathbf{M}^L) \cdot \{1, 0\} = \{0, 0\}$.) For $n \geq 3$, we have (cf. Refs. [21,22], see also Ref. [42], in which a recursive formula for a different object was obtained)

$$\mathbf{N}^{(n)}(\chi_0, \sigma) = \int_\sigma^\infty \frac{\mathrm{d}\sigma'}{\chi_0} \int_0^1 \mathrm{d}q \{\mathbf{M}^L(\chi, q) \cdot \mathbf{N}^{n-1}(\chi_0, \sigma') + \mathbf{M}^C(\chi, q) \cdot \mathbf{N}^{(n-1)}([1-q]\chi_0, \sigma')\}. \quad (7)$$

$1 - q$ accounts for the recoil due to photon emission. The trident probability is obtained by resumming the α expansion, $P = \mathbf{N}_0 \cdot \mathbf{N}(\chi_0, -\infty)$, where $\mathbf{N}_0$ describes the spin of the initial electron and

$$\mathbf{N}(\chi_0, \sigma) = \sum_{n=2}^\infty T^n \mathbf{N}^{(n)}(\chi_0, \sigma), \quad (8)$$

where $T = a_0\alpha$. $\mathbf{N}(\chi_0, \sigma)$ can be obtained either 1) by calculating the first, e.g., 10, terms, $\mathbf{N}^{(2)}$ to $\mathbf{N}^{(11)}$, and then resumming them with some appropriate method (see below) or 2) by resumming before computing, i.e., solving the following integrodifferential[6] equation:

$$\frac{\partial \mathbf{N}}{\partial \sigma} = T^2 \frac{\partial \mathbf{N}^{(2)}}{\partial \sigma} - T \int_0^1 \frac{\mathrm{d}q}{\chi_0} \{\mathbf{M}^L \cdot \mathbf{N}(\chi_0) + \mathbf{M}^C \cdot \mathbf{N}([1-q]\chi_0)\}. \quad (9)$$

We integrate this backward in time starting with $\mathbf{N}(\chi_0, +\infty) = \{0, 0\}$. Note that, while (7) has the same form as Eq. (1) in Ref. [21], Eq. (9) has an extra, inhomogeneous term compared to Eq. (2) in Ref. [21].

III. CONSTANT FIELD

For a constant field, the σ integrals simply give $\int \mathrm{d}\sigma_1 \ldots \mathrm{d}\sigma_n = \Delta\sigma^n/n!$, with $n!$ due to time ordering. It is natural to absorb $\Delta\sigma$ into $T = \Delta\sigma a_0 \alpha$. Hence, Eq. (7) reduces to

[5] In the literature, ξ is another common symbol for what we call a_0. We never use ξ for a_0.

[6] Integrodifferential equations, for different objects, also appear in macroscopic, kinetic approaches; see, e.g., Refs. [43–46].

$$\mathbf{N}^{(n)} = \int_0^1 \frac{dq}{n\chi}\{\mathbf{M}^C \cdot \mathbf{N}^{(n-1)}(\chi[1-q]) + \mathbf{M}^L \cdot \mathbf{N}^{(n-1)}(\chi)\}. \tag{10}$$

We can now use T rather than σ as variable for an integrodifferential equation. We find (with arguments of $\mathbf{M}^{C,L}$ suppressed)

$$\frac{\partial}{\partial T}\mathbf{N}(T,\chi) = 2T\mathbf{N}^{(2)}(\chi) + \int_0^1 \frac{dq}{\chi}\{\mathbf{M}^C \cdot \mathbf{N}(T,\chi[1-q]) + \mathbf{M}^L \cdot \mathbf{N}(T,\chi)\}, \tag{11}$$

with "initial" condition $\mathbf{N}(0,\chi) = \{0,0\}$. The final results are shown in Figs. 2–4, which show perfect agreement between the results obtained from (11) and from (23).

A. Leading contribution in $\chi \ll 1$

For $\chi \ll 1$ and a constant field, we find (see Appendix A)

$$\mathbf{N}^{(n)} \approx \{a_n, \chi b_n\} \exp\left(-\frac{16}{3\chi}\right), \tag{12}$$

where

$$a_2 = \frac{1}{2}\frac{1}{32} \qquad b_2 = \frac{1}{2}\frac{1}{32\times 27} \tag{13}$$

and

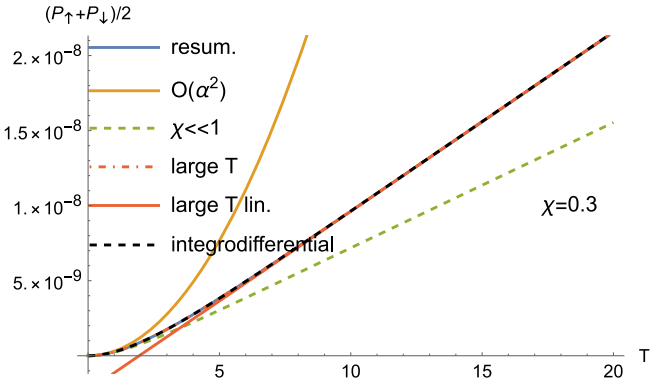

FIG. 2. Trident pair production resummed to all orders in α. The initial electron has spin up or down along the magnetic field, $P_\downarrow$ and $P_\uparrow$, and $T = \Delta\sigma a_0 \alpha$. The "resum." line is obtained by resumming the χ expansion with Padé-Borel and the α expansion with the resummation method in (23), with $n = 1$ in (26). The "integrodifferential" line is a numerical solution to (11). The $\mathcal{O}(\alpha^2)$ line gives the trident probability with no RR. The $\chi \ll 1$ line gives the low-energy limit in (15). The "large T lin." line shows the pure large-T limit (C1). The "large T" line is the improvement in (C7).

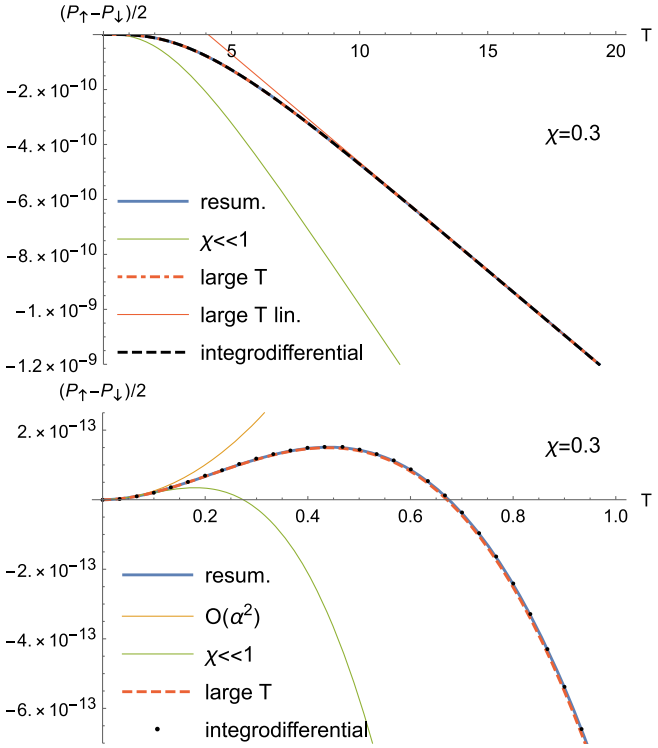

FIG. 3. Similar to Fig. 2 but for $(P_\downarrow - P_\uparrow)/2$, with Padé approximant as in (26) with $n = 2$. The $\chi \ll 1$ line gives the low-energy limit in (16).

$$a_n = \frac{2(-d)^{n-2}}{n!}a_2$$
$$b_n = \frac{2(-d)^{n-2}}{n!}\left(b_2 + \frac{f}{d}(n-2)a_2\right), \tag{14}$$

where $d \approx 0.711201$ and $f \approx 0.419148$. Thus, for an initial electron with spin up or down, we find

$$\langle P\rangle = \frac{P_\uparrow + P_\downarrow}{2} = \{1,0\}\cdot\sum_{n=2}^{\infty} T^n \mathbf{N}^{(n)} \approx e^{-\frac{16}{3\chi}}\sum_{n=2}^{\infty} a_n T^n = \frac{T^2 F(dT)}{2\times 32}\exp\left(-\frac{16}{3\chi}\right), \tag{15}$$

$$\frac{P_\uparrow - P_\downarrow}{2} = \{0,1\}\cdot\sum_{n=2}^{\infty} T^n \mathbf{N}^{(n)} \approx \chi e^{-\frac{16}{3\chi}}\sum_{n=2}^{\infty} b_n T^n = \left(\frac{1}{27}F(dT) - \frac{f}{d}G(dT)\right)\frac{T^2}{64}\chi\exp\left(-\frac{16}{3\chi}\right), \tag{16}$$

where

$$F(x) = \frac{2}{x^2}[e^{-x} - 1 + x] \tag{17}$$

and

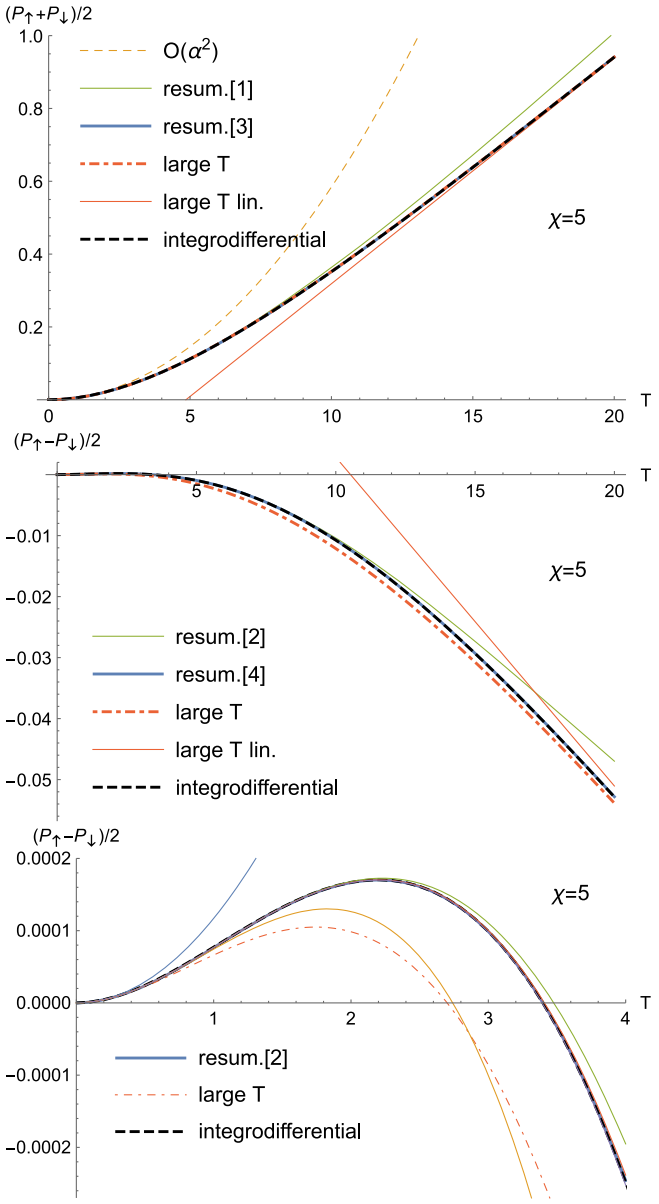

FIG. 4. As Figs. 2 and 3 but with $\chi = 5$. n in "resum.[n]" refers to the Padé order in (26). The thin solid lines in the last plot show the result of a direct summation (i.e., with no resummation) of the α expansion; summing more than the first four or five terms gives lines that agree, on the scale of that plot, with the results from resummation or from the integrodifferential equation.

$$G(x) = \frac{2}{x^2}[x - 2 + (2 + x)e^{-x}]. \tag{18}$$

For $T \ll 1$, the resummation reduces to trident at $\mathcal{O}(\alpha^2)$, but for $T \gg 1$, the probability grows linearly, $P \sim T$. We can understand this as follows. The intermediate photon can decay anywhere in the field, which gives a volume factor T. Without RR, the electron can emit that photon anywhere in the pulse, which gives another factor of T. However, with RR, the electron's longitudinal momentum decreases over time, so the electron can only emit (with significant probability) a sufficiently high-energy photon during a limited time interval; i.e., there is no additional factor of T.

We find that $P_\uparrow - P_\downarrow$ changes sign as T increases and that this happens already at $T \sim 0.3$. Thus, from the $\mathcal{O}(\alpha^2)$ results, we have that $P_\uparrow > P_\downarrow$ for $T \ll 1$, but as T increases, we instead find $P_\downarrow > P_\uparrow$, and a_0 actually does not have to be extremely large for this to happen.

IV. RESUMMING CONVERGENT SERIES

In Refs. [21,22], we found α expansions which seem to have finite radius of convergence, which we therefore resummed with Padé approximants. In contrast, in (15) and (16), we see an infinite radius. In principle, one can sum such series directly without any resummation. But that would mean having to calculate more and more terms to reach convergence as we increase T (see Fig. 5). This is neither efficient nor practical because, in contrast to (14), we will in general only be able to obtain a finite number of terms, up to $\mathcal{O}(\alpha^{n_{\max}})$ for some $n_{\max}$, and only to finite precision. A direct sum, $\sum_{n=0}^{n_{\max}} T^n \mathbf{N}^{(n)}$, scales as $T^{n_{\max}}$ as $T \to \infty$, which is not physical since $n_{\max}$ is just the order where we happened to stop. Thus, we still need to resum this type of series. But Padé or Borel-Padé resummations are only suitable for series with finite or zero radius of convergence. To find a suitable method, it still helps to recall that in the Borel-Padé method, one divides the coefficients by $n!$ to turn the original series into one with finite radius of convergence, which can then be resummed with Padé approximants (see Appendix B). In our case, we have series on the form

$$\psi(x) = \sum_{n=0}^{\infty} c_n x^n, \tag{19}$$

where $|c_n| \sim 1/n!$ at large n. We turn such a series into one with finite radius of convergence by instead multiplying the coefficients c_n by $n!$. This, of course, gives the expansion of a different function. The key to transforming back to the original function is the "Hankel's loop integral" (see Eq. (5.9.2) in Ref. [47])

$$1 = n! \int_\gamma \frac{\mathrm{d}t}{2\pi i} e^t t^{-(1+n)}, \tag{20}$$

where γ starts at $t = -\infty - i\epsilon$, wraps around the negative real axis, and ends at $t = -\infty + i\epsilon$. We can then write[7]

[7]We refrain from calling this the "Hankel transform" since that name is already used for something else.

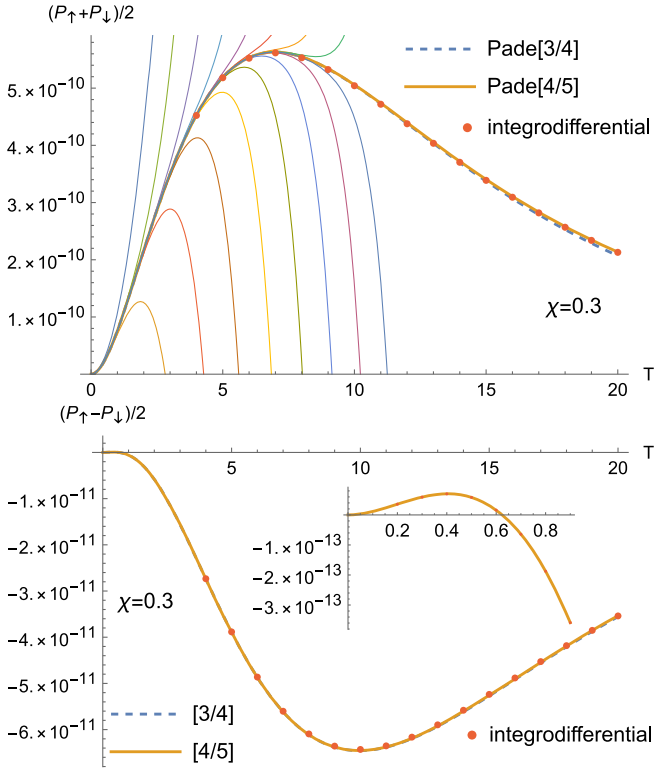

FIG. 5. Similar to Fig. 2 but for a Sauter pulse and with $T = a_0\alpha$. The thin lines for $(P_\downarrow + P_\uparrow)/2$ show the results of just adding the n terms $\mathcal{O}(\alpha^2)$ to $\mathcal{O}(\alpha^{n+1})$ without any resummation. The $[m/m+1]$ lines are obtained with the method using the transform in (21), and the dots are solutions to (9).

$$\psi(x) = \int_\gamma \frac{\mathrm{d}t}{2\pi i}\frac{e^t}{t} H\psi(x/t) \qquad H\psi(z) = \sum_{n=0}^{\infty} n! c_n z^n. \tag{21}$$

Since $|c_n| \sim 1/n!$ at large n, $H\psi(z)$ has a finite radius of convergence. We can therefore resum the truncated transform

$$H\psi_{n_{\max}}(z) = \sum_{n=0}^{n_{\max}} n! c_n z^n \tag{22}$$

by matching it onto a Padé approximant [e.g., Eq. (26)]. The final resummation is thus given by

$$\psi(x) = \int_\gamma \frac{\mathrm{d}t}{2\pi i}\frac{e^t}{t} PH\psi(x/t), \tag{23}$$

where the integral can be performed with the residue theorem.

To check that this method works, we consider first the low-energy limit of $\langle P\rangle$, for which we have $\psi = \sum_{n=2}^{\infty} a_n T^n$ with a_n given by (14). For this example, we find a simple geometric series for $H\psi$,

$$H\psi = 2a_2T^2 \sum_{n=2}^{\infty} \frac{(-dT)^{n-2}}{t^n} = \frac{2a_2T^2}{t(t+dT)}. \tag{24}$$

The radius of convergence of this series is $|dT/t| < 1$, so it makes sense to choose the integration contour γ such that $|t| > dT$. We can now perform the t integral with the residue theorem. We have poles at $t = 0$ and $t = -dT$, and they both contribute. We find

$$\psi(x) = \int_\gamma \frac{\mathrm{d}t}{2\pi i}\frac{e^t}{t} H\psi = a_2T^2F(dT), \tag{25}$$

which agrees with (15). We also recover (16) in the same way. In these examples, we have access to all terms, and we find geometric series that can be resummed as in (24), which is already exactly the ratio of two polynomials. The point is that in general, beyond the leading $\chi \ll 1$ limit, we will not find a geometric series, but we can still resum the $H\psi$ series with Padé approximants.

For a constant field, we have a T^2 scaling at $T \ll 1$ and expect linear scaling for large T, so we choose $[n+1/n]$ Padé approximants as

$$PH\psi(z) = \frac{\sum_{i=2}^{n+1} A_i z^i}{1 + \sum_{j=1}^{n} B_j z^j}. \tag{26}$$

Results are shown in Figs. 2 and 3. The convergence is very fast. For $\chi = 0.3$, we only need $n = 1$ and $n = 2$ for the unpolarized and polarized parts; i.e., we only need terms up to $\mathcal{O}(\alpha^3)$ and $\mathcal{O}(\alpha^5)$. Note that for $n = 1$, we have exactly the same functional dependence of T as in (15), and only the overall coefficient and the constant d are different. There is, however, no reason to expect that $n = 1$ and $n = 2$ would be enough if we consider larger χ. But it turns out that we actually have to increase χ significantly to see this.

In Fig. 4, we show plots similar to Figs. 2 and 3 but for $\chi = 5$. One cannot actually neglect multiple pair production and other terms (multiple polarization/fermion loops) with similar exponential scalings for such a large χ, which is obvious since the result for the probability is close to 1. We present these results just to show the power of the resummation methods. In Fig. 4, we can start to see a significant error at larger T for $n = 1, 2$ in (26). However, here we have increased χ so much that the results are no longer physical, and even then, the errors are not huge, so when we consider smaller χ (where we can neglect the fermion loops), the errors will be quite small. Thus, if we stick to a regime where our current approach gives physical results, then we find that we need very few terms from the α expansion to reach convergence.

The final result obtained by performing the integral in (23) with the residue theorem is a sum of products of polynomials and exponentials ($e^{-\mathrm{const}\,T}$) similar to the low-energy limit in (15) and (16). If one can guess some appropriate order of these polynomials and the number of

different exponentials, then one can of course obtain the coefficients by directly matching with the T expansion, i.e., without introducing the Hankel integral. However, for the examples we have tried, it seems to be much easier to obtain a good resummation by first making this transformation.

Recall that Padé approximants can have spurious poles, and note that, in general, we can only obtain the α expansion to a finite precision. We have in some cases found that this method can give terms with $e^{+\text{const}\,T}$, where $\text{Re}(\text{const}) > 0$, but with a numerically very small preexponential factor which makes this unphysical T scaling nevertheless negligible for reasonably large T. For larger T, one can try to fix such cases by simply removing the terms with $e^{+\text{const}\,T}$. If the corresponding preexponential coefficients are several orders of magnitude smaller than the coefficients in front of terms with $e^{-\text{const}\,T}$, then one can expect that the $T \ll 1$ expansion of ψ_{fix} is still correct to a good precision. Without this fix, the expansion of ψ_{resum} will agree with $\mathbf{N}^{(n)}$, $n \leq n_{\text{max}}$, to within the working precision (e.g., 10^{-15}). But if we only know $\mathbf{N}^{(n)}$ with a precision of, e.g., 10^{-5}, then it is not a problem if ψ_{fix} only agrees with $\mathbf{N}^{(n)}$ to a precision of 10^{-5}. While this fix seems to work well, it still leaves some inspiration for trying to find more optimal use of the n_{max} terms calculated. In any case, this has not been a problem for the cases shown in the plots.

V. RESULTS FOR A SAUTER PULSE

As an example of a pulsed field, we consider a Sauter pulse[8] $a_\mu(\sigma) = \delta_{\mu 1} a_0 \tanh(\sigma)$. The results are shown in Fig. 5. We have used (7) to obtain the first $\gtrsim$10 terms and resummed them using the method described above. In Fig. 6, we plot the ratios of neighboring coefficients in the α expansion for the Sauter pulse case and with $\chi = 0.3$. From this, we can see that multiplying the coefficients by $n!$ indeed seems to give a series with finite radius of convergence. Here, too, we find that $(P_\uparrow - P_\downarrow)/2$ changes sign as T increases and that this happens already for $T < 1$. In contrast to the constant-field case, here P decreases as $T \to \infty$. It is therefore better to choose $[n/n+1]$ approximants rather than (26), to remove the pole at $t = 0$, which would otherwise give terms without exponential suppression. The results agree with the solution to (9). We can understand the different asymptotic scaling roughly as follows.[9] We model the exponential suppression of pair production by $e^{-\text{const}/\chi(\sigma)}$, where $\chi(\sigma) =$

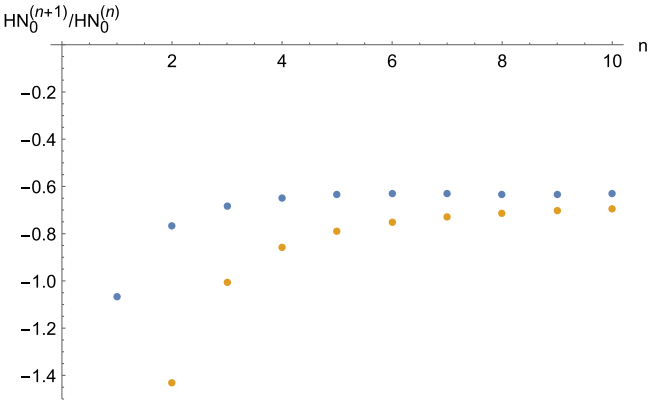

FIG. 6. Ratios of neighboring coefficients of $HN_0^{(n)} \coloneqq n!\{1,0\} \cdot \mathbf{N}^{(n)}$ for a Sauter pulse and $\chi = 0.3$.

$kP(\sigma)a_0 f'(\sigma)$ is the product of a local field strength $a_0 f'(\sigma)$ and a local momentum $kP(\sigma)$, which we estimate using the solution to the Landau-Lifshitz equation [52,53], $kP(\sigma) \to b_0/(1 + [2/3]Ta_0 \int_{-\infty}^{\sigma} \mathrm{d}\sigma f'(x))$. $kP(\sigma)$ decreases and hence favors production early in the pulse, while $a_0 f'(\sigma)$ favors production close to the field maximum. For a constant field, $f' = 1$, only $kP(\sigma)$ is relevant, and the dominant contribution comes from the time just after the electron has entered the field and before it has lost too much momentum, which gives a T-independent exponent, $e^{-\text{const}/\chi(-\infty)}$. For a Sauter pulse, $f'(\sigma) = \text{sech}^2(\sigma)$, the dominant contribution comes instead from $\chi'(\sigma_d) = 0$, giving $\sigma_d = -(1/4)\ln[1 + (4/3)a_0 b_0 T]$, and $e^{-\text{const}/\chi(\sigma_d)} \sim e^{-\text{const}'T}$ as $T \to \infty$. This difference does not make the constant field irrelevant for large T. We show, e.g., in Appendix D that a circularly polarized monochromatic field also leads to (15), but with different coefficients.

VI. CONCLUSIONS AND OUTLOOK

In conclusion, we have derived recursive and integro-differential matrix equations for calculating the probability of nonlinear trident to all orders in α. We have shown that corrections to $\mathcal{O}(\alpha^2)$ become important already for values of $T = a_0\alpha$ that can be generated with today's lasers. We have also found a new transform for resumming convergent series, of which the α expansion of trident is one example. We have focused on $a_0 \gg 1$, but these methods can be used even if $a_0 \sim 1$, provided one uses the appropriate Mueller matrices in Refs. [38,39] and the pulse is long. For general spin/polarization, one would have to take into account vacuum birefringence on the intermediate photon, i.e., by resumming the loops between A and B in Fig. 1 as in Ref. [38]. It would also be interesting to consider the spin of the produced positron. This has been studied using PIC codes in Refs. [49,50,54]. For that, we would need to take RR into account on the positron line (connected to B in Fig. 1), e.g., by finding a recursive formula similar to (7).

[8]Oscillations in the field tend to average out spin effects. This can be avoided by making the oscillations asymmetric [48,49] or by using dense electron beams to generate nonoscillating fields [50].

[9]Using similar estimates and particle-in-cell (PIC) simulations, Ref. [51] also found pair production maximized at a finite pulse length (but for an oscillating field and a different pulse envelope).

When planning such generalizations, it is encouraging to note that we have been able to resum the α expansions both in this paper and in Refs. [21,22] with relatively few terms.

ACKNOWLEDGMENTS

G. T. is supported by the Swedish Research Council, Contract No. 2020-04327.

APPENDIX A: χ-EXPANSION APPROACH

In this section, we will explain how to obtain the constant-field results by making a second expansion, i.e., by expanding each order in α in an asymptotic expansion in χ. We work backward, starting with the pair-production step.

To obtain the χ expansions, we need the following expansions of the Airy functions. Let $\gamma = r/\chi$. For large γ, we can obtain an expansion of $\mathrm{Ai}_1(\gamma^{2/3})$ by first writing it in terms of the following integral representation,

$$\mathrm{Ai}_1(\gamma^{2/3}) = \frac{i}{2\pi}\int_{-\infty}^{\infty}\frac{\mathrm{d}\tau}{\tau}\exp\left\{i\gamma\left(\tau+\frac{\tau^3}{3}\right)\right\}, \quad \text{(A1)}$$

where the integration contour passes above the pole. We can now obtain an expansion using the saddle-point method; i.e., we change variable from $\tau = i + (1/\sqrt{\gamma})\delta\tau$ to $\delta\tau$, expand the integrand in a series in $1/\gamma$, and perform the resulting Gaussian integrals. We find

$$\mathrm{Ai}_1(\gamma^{2/3}) = \frac{\exp\left(-\frac{2\gamma}{3}\right)}{2\sqrt{\pi\gamma}}\left(1-\frac{41}{48\gamma}+\frac{9241}{4608\gamma^2}+\ldots\right), \quad \text{(A2)}$$

where we can quickly obtain the next > 100 terms. The corresponding expansion for $\mathrm{Ai}'(\gamma^{2/3})/\gamma^{2/3}$ can be obtained directly from the known expansion of the Airy function, and one finds

$$\frac{\mathrm{Ai}'(\gamma^{2/3})}{\gamma^{2/3}} = -\frac{\exp\left(-\frac{2\gamma}{3}\right)}{2\sqrt{\pi\gamma}}\left(1+\frac{7}{48\gamma}-\frac{455}{4608\gamma^2}+\ldots\right). \quad \text{(A3)}$$

To obtain an expansion for the pair-production probability integrated over the longitudinal momentum, we first change variables from s_3 to $r = (1/[1-s_3]) + (1/s_3)$. Due to $\exp(-2r/[3\chi])$, the integrand can be expanded around the minimum of r, which is $r = 4$. We therefore change variable from $r = 4 + \chi R^2$ to R. Expanding the integrand in a series in χ gives integrals on the form

$$\int_0^\infty \mathrm{d}R\, R^n \exp\left(-\frac{2}{3}R^2\right) = \frac{\Gamma\left[\frac{3}{2}+\frac{n}{2}\right]}{(2/3)^{(1+n)/2}(1+n)}. \quad \text{(A4)}$$

We thus obtain

$$T\mathbf{N}^{(1)} = T\frac{3}{16}\sqrt{\frac{3}{2}}\exp\left(-\frac{8}{3\chi}\right) \times\left\{1-\frac{11\chi}{64}+\frac{7985\chi^2}{73728}+\ldots, -\frac{1}{3}+\frac{65\chi}{576}-\frac{21361\chi^2}{221184}\ldots\right\}. \quad \text{(A5)}$$

The probability for nonlinear Breit-Wheeler pair production is given by $P = \mathbf{N}_\gamma \cdot T\mathbf{N}^{(1)}$, where $T = \alpha a_0 \Delta\phi$. To leading order, we recognize the fact that a perpendicularly polarized photon gives twice as large probability compared to a parallel photon, i.e., $\{1,-1\}\cdot\mathbf{N}^{(1)} \approx 2\{1,1\}\cdot\mathbf{N}^{(1)}$; see Refs. [55–57] for the constant-crossed field and Ref. [58] for a general pulsed plane wave.

Now that we have obtained $\mathbf{N}^{(1)}$, the next step is to prepend $\mathbf{M}^C_{0\gamma}$ as in (4) and calculate a corresponding expansion. $\chi = a_0 kl$ in (A5) where l_μ is the intermediate photon momentum. When we prepend $\mathbf{M}^C_{0\gamma}$, we change notation by replacing $\chi = a_0 kl = a_0(kl/kp)kp \to q\chi$, where now $\chi = a_0 kp$ and p_μ is the momentum of the electron before emitting the intermediate photon. The intermediate photon needs to have sufficiently high energy in order to produce a pair, so the probability to emit such a photon also has an exponential expansion similar to (A5). We obtain this using (A5) and an expansion of (3). For the exponential part of the q integral, we have

$$\exp\left\{-\frac{2}{3}(\gamma_2+\gamma_1)\right\}, \quad \text{(A6)}$$

where $\gamma_1 = 4/(q\chi)$ comes from (A5), and from (3), we have $\gamma_2 = r/\chi$ with $r = (1/s_1) - 1$ and $s_1 = 1 - q$. There is a saddle point at $q = 2/3$, which corresponds to the point where all three final-state fermions have the same momentum, i.e., $s_1 = s_2 = s_3 = 1/3$ and $q = 1 - s_1 = s_2 + s_3$. In principle, we could change variable from $q = (2/3) + \sqrt{\chi}\delta q$ to δq and expand the integrand in a series in χ. However, to obtain a large number of terms in the χ expansion, it seems faster to instead change variables from

$$q = \frac{24+3\chi W^2+\sqrt{3\chi}W\sqrt{16+3\chi W^2}}{6(6+\chi W^2)} \quad \text{(A7)}$$

to W, where $W(q=0) = -\infty$ and $W(q=1) = +\infty$, which is useful because then the exponent becomes exactly Gaussian,

$$\exp\left\{-\frac{2}{3}(\gamma_2+\gamma_1)\right\} = \exp\left\{-\frac{16}{3\chi}-W^2\right\}, \quad \text{(A8)}$$

which means we do not have to expand the exponential part of the integrand in a series in χ. We thus obtain

$$T^2\mathbf{N}^{(2)} = \frac{T^2}{2}\frac{\exp\left(-\frac{16}{3\chi}\right)}{32} \times \left\{1 + \frac{31\chi}{216} - \frac{3871\chi^2}{31104} + \cdots, \frac{\chi}{27} - \frac{37\chi^2}{972} + \cdots\right\}. \tag{A9}$$

The probability of trident pair production to leading order in α is given by $P = \mathbf{N}_0 \cdot T^2\mathbf{N}^{(2)}$, where $\mathbf{N}_0$ is the Stokes vector of the initial electron. The expansion of the unpolarized part, i.e., $\{1,0\}\cdot\mathbf{N}^{(2)}$, agrees with what we found in Ref. [14]. In order to go beyond the leading order in α, we also need the part that describes the dependence on the spin of the initial electron, i.e., $\{0,1\}\cdot\mathbf{N}^{(2)}$. The leading term in this part, i.e., the one proportional to $\chi/27$, agrees with Eq. (24) in Ref. [3] and Eq. (92) in Ref. [39].[10] Here, we have calculated the first $\sim$100 terms in the χ expansion.

We obtain the χ expansions of $\mathcal{O}(\alpha^3)$ and higher orders in α using (10) with the χ expansion of $\mathbf{N}^{(2)}$ as input. To obtain the $\chi \ll 1$ expansion of these orders, we need the following integrals. We change variables in (10) from $q = \chi\gamma/(1+\chi\gamma)$ to $\gamma = r/\chi$, where $r = (1/s_1) - 1$ and $s_1 = 1 - q$. From terms with $\mathbf{M}^L$, we have the same integrals as in Ref. [21], i.e.,

$$\mathcal{I}_{\mathrm{Ai}}(n) = \int_0^\infty \mathrm{d}\gamma\, \gamma^n \frac{\mathrm{Ai}(\gamma^{2/3})}{\gamma^{1/3}} = \frac{3^{\frac{1}{2}+n}}{4\pi}\Gamma\left[\frac{1}{3}+\frac{n}{2}\right]\Gamma\left[\frac{2}{3}+\frac{n}{2}\right], \tag{A10}$$

$$\mathcal{I}_{\mathrm{Ai}'}(n) = \int_0^\infty \mathrm{d}\gamma\gamma^n \frac{\mathrm{Ai}'(\gamma^{2/3})}{\gamma^{2/3}} = -\frac{3^{\frac{1}{2}+n}}{4\pi}\Gamma\left[\frac{1}{6}+\frac{n}{2}\right]\Gamma\left[\frac{5}{6}+\frac{n}{2}\right], \tag{A11}$$

$$\mathcal{I}_{\mathrm{Ai}_1}(n) = \int_0^\infty \mathrm{d}\gamma\gamma^n \mathrm{Ai}_1(\gamma^{2/3}) = \frac{3^{\frac{1}{2}+n}}{2\pi(1+n)}\Gamma\left[\frac{5}{6}+\frac{n}{2}\right]\Gamma\left[\frac{7}{6}+\frac{n}{2}\right]. \tag{A12}$$

From terms with $\mathbf{M}^C$, we have $\exp(-16/[3(1-q)\chi]) = \exp(-16/[3\chi] - 16\gamma/3)$, which leads to the following integrals,

$$\{\mathcal{J}_{\mathrm{Ai}_1}, \mathcal{J}_{\mathrm{Ai}}, \mathcal{J}_{\mathrm{Ai}'}\} = \int_0^\infty \mathrm{d}\gamma\gamma^n e^{-c\gamma}\left\{\mathrm{Ai}_1(\gamma^{2/3}), \frac{\mathrm{Ai}(\gamma^{2/3})}{\gamma^{1/3}}, \frac{\mathrm{Ai}'(\gamma^{2/3})}{\gamma^{2/3}}\right\}, \tag{A13}$$

where $c = 16/3$. With

$$\left\{\mathrm{Ai}_1(\gamma^{2/3}), \frac{\mathrm{Ai}(\gamma^{2/3})}{\gamma^{1/3}}, \frac{\mathrm{Ai}'(\gamma^{2/3})}{\gamma^{2/3}}\right\} = \int \frac{\mathrm{d}\tau}{2\pi}\left\{\frac{i}{\tau}, 1, i\tau\right\}\exp\left[i\gamma\left(\tau + \frac{\tau^3}{3}\right)\right], \tag{A14}$$

we find

$$\{\mathcal{J}_{\mathrm{Ai}_1}, \mathcal{J}_{\mathrm{Ai}}, \mathcal{J}_{\mathrm{Ai}'}\} = n!\int \frac{\mathrm{d}\tau}{2\pi}\left\{\frac{i}{\tau}, 1, i\tau\right\}\left[c - i\left(\tau + \frac{\tau^3}{3}\right)\right]^{-(1+n)}. \tag{A15}$$

These integrals can now be performed with the residue theorem. We close the contour in the upper-half complex plane, where there is one pole at

$$\tau_p = i\left[(8+3\sqrt{7})^{1/3} + \frac{1}{(8+3\sqrt{7})^{1/3}}\right]. \tag{A16}$$

To simplify the calculation of the residue for large n, we first perform partial integration

$$\{\mathcal{J}_{\mathrm{Ai}_1}, \mathcal{J}_{\mathrm{Ai}}, \mathcal{J}_{\mathrm{Ai}'}\} = \int \frac{\mathrm{d}\tau}{2\pi}\left[c - i\left(\tau + \frac{\tau^3}{3}\right)\right]^{-1}\left[\frac{\partial}{\partial\tau}\frac{i}{(1+\tau^2)}\right]^n\left\{\frac{i}{\tau}, 1, i\tau\right\} = \mathcal{J}_{\mathrm{Ai}}(n=0)\left[\frac{\partial}{\partial\tau}\frac{i}{(1+\tau^2)}\right]^n\left\{\frac{i}{\tau}, 1, i\tau\right\}\Big|_{\tau=\tau_p}, \tag{A17}$$

where $[\ldots]^n$ means $[\ldots][\ldots]\ldots[\ldots]$ with the derivatives acting on everything on the right. For $n = 0, 1, 2, \ldots$, we have

$$\begin{aligned}\mathcal{J}_{\mathrm{Ai}_1} &= \{0.0458131, 0.00685688, 0.00211075, \ldots\}\\ \mathcal{J}_{\mathrm{Ai}} &= \{0.133495, 0.0138645, 0.00368465, \ldots\}\\ -\mathcal{J}_{\mathrm{Ai}'} &= \{0.388994, 0.0225791, 0.00518418, \ldots\}.\end{aligned} \tag{A18}$$

These numbers can actually be expressed as the roots of third-order polynomials with integer coefficients, e.g.,

$$-1 + 3\mathcal{J}_{\mathrm{Ai}}(0) + 252\mathcal{J}_{\mathrm{Ai}}^3(0) = 0, \tag{A19}$$

but it is faster to express them in decimal form. Since precision is often lost in the resummations we are doing, we start with many more digits than those presented in (A18).

$\{\mathcal{J}_{\mathrm{Ai}_1}, \mathcal{J}_{\mathrm{Ai}}, \mathcal{J}_{\mathrm{Ai}'}\}$ grow factorially fast as $n \to \infty$. To obtain this limit, we write

[10] Our $\hat{B}$ corresponds to $-\mathbf{e}_2$ [39] as explained in Eq. (52) in Ref. [38].

$$\{\mathcal{J}_{\mathrm{Ai}_1},\mathcal{J}_{\mathrm{Ai}},\mathcal{J}_{\mathrm{Ai}'}\} = n!\int\frac{\mathrm{d}\tau}{2\pi}\left\{\frac{i}{\tau},1,i\tau\right\} \times\exp\left\{-(1+n)\ln\left[c-i\left(\tau+\frac{\tau^3}{3}\right)\right]\right\} \tag{A20}$$

and then perform the integral with the saddle-point method; i.e., we change variable from $\tau = i + (1/\sqrt{n})\delta\tau$ to $\delta\tau$ and expand the integrand in a series in $1/n$. We obtain

$$\begin{aligned}&\{\mathcal{J}_{\mathrm{Ai}_1},\mathcal{J}_{\mathrm{Ai}},-\mathcal{J}_{\mathrm{Ai}'}\}\\ &=\frac{\Gamma(n+\frac{1}{2})}{2\sqrt{6\pi}6^n}\left\{1-\frac{41}{8n}+\frac{8913}{128n^2}-\frac{4635593}{3072n^3}+\cdots,\right.\\ &\quad 1-\frac{5}{8n}+\frac{345}{128n^2}-\frac{67085}{3072n^3}+\cdots,\\ &\quad\left.1+\frac{7}{8n}-\frac{399}{128n^2}+\frac{73927}{3072n^3}+\cdots\right\}.\end{aligned} \tag{A21}$$

Thus, starting with (A9) and repeatedly using (10), we find, for $n = 3$ up to some $n_{\max}$ where we decide to stop,

$$\mathbf{N}^{(n)} = \exp\left(-\frac{16}{3\chi}\right)\left\{\sum_{m=0}^{m_{\max}}a_m^{(n)}\chi^m,\sum_{m=1}^{m_{\max}}b_m^{(n)}\chi^m\right\}, \tag{A22}$$

where the coefficients grow factorially with alternating sign, $a_m^{(n)}, b_m^{(n)} \propto (-1)^m m!$ for $m\to\infty$. Note that the χ expansion of $\mathbf{N}^{(n)}$ is obtained by inserting the unresummed χ expansion of $\mathbf{N}^{(n-1)}$ into (10). We have calculated $n_{\max} = \mathcal{O}(10)$ and $m_{\max} = \mathcal{O}(100)$ terms. We first resum the χ expansion of each order in α, with Borel-Padé as explained in Appendix B, before we resum the α expansion with the method in Sec. IV. The results are shown in Figs. 2–4.

To leading order in $\chi \ll 1$, we can obtain a compact, explicit form for the coefficients to all orders in α, i.e., without stopping at some finite $n_{\max}$. We obtain this by starting with the ansatz

$$\mathbf{N}^{(n)} = \{a_n + \chi c_n, \chi b_n\}\exp\left(-\frac{16}{3\chi}\right), \tag{A23}$$

where a_n and b_n are constants. At $n = 2$, we have

$$a_2 = \frac{1}{2}\frac{1}{32} \qquad b_2 = \frac{1}{2}\frac{1}{32\times 27}. \tag{A24}$$

It turns out that we do not need c_n in order to obtain a_n and b_n. We find

$$a_n = -\frac{d}{n}a_{n-1} \qquad b_n = -\frac{1}{n}[f a_{n-1} + d b_{n-1}], \tag{A25}$$

where

$$\begin{aligned}d &= \mathcal{J}_{\mathrm{Ai}_1}(0) + 2\mathcal{J}_{\mathrm{Ai}'}(0) - \mathcal{I}_{\mathrm{Ai}_1}(0) - 2\mathcal{I}_{\mathrm{Ai}'}(0)\\ &\approx 0.711201\end{aligned} \tag{A26}$$

and

$$f = \mathcal{I}_{\mathrm{Ai}}(1) - \mathcal{J}_{\mathrm{Ai}}(1) \approx 0.419148. \tag{A27}$$

This gives us (14).

APPENDIX B: BOREL RESUMMATION

The χ expansions discussed above are asymptotic and can be resummed with the Borel-Padé method [59–68]. There are other methods that can be more efficient [69–71], i.e., which require fewer terms to reach convergence. However, here we can without problem obtain a large number of terms in the χ expansions, so the standard Borel-Padé method is enough. We will give a short summary of this method here. Another reason for doing so is to compare and contrast with the resummation method of convergent series in Sec. IV.

An asymptotic series is given by

$$\psi(x) = \sum_{n=0}^{\infty} c_n x^n, \tag{B1}$$

where $|c_n| \sim n!$ at large n. To resum this, one can insert

$$1 = \frac{1}{n!}\int_0^\infty \mathrm{d}t\, t^n e^{-t} \tag{B2}$$

into the summand (B1),

$$\psi(x) = \int_0^\infty \mathrm{d}t\, e^{-t} B\psi(xt), \tag{B3}$$

where

$$B\psi(xt) = \sum_{n=0}^{\infty}\frac{c_n}{n!}(xt)^n \tag{B4}$$

is the Borel transform. In the problems we are interested in, we usually only have access to a finite number of terms, but $B\psi$ as a finite radius of convergence so the truncated transform

$$B\psi_N(t) = \sum_{n=0}^{N}\frac{c_n}{n!}t^n \tag{B5}$$

can be resummed by matching it onto a Padé approximant,

$$PB\psi(t) = \frac{\sum_{i=0}^{I}A_i t^i}{1+\sum_{j=1}^{J}B_j t^j}, \tag{B6}$$

where the coefficients A_i and B_j are determined by demanding that

$$PB\psi(t) = B\psi_N(t) + \mathcal{O}(t^{N+1}). \tag{B7}$$

One can choose different I and J depending on the problem, but $I = J$ or $I \approx J$ are often good choices. The final resummed result is then given by

$$\psi(x) = \int_0^\infty \mathrm{d}t\, e^{-t} PB\psi(xt). \tag{B8}$$

APPENDIX C: LARGE T LIMIT

For a constant field, we can obtain the large T results approximately by substituting the ansatz

$$\mathbf{N}(T,\chi) \approx T\mathbf{N}^L(\chi) + \mathbf{N}^{NL}(\chi) \tag{C1}$$

into (11). The leading order is then determined by

$$\int_0^1 \frac{\mathrm{d}q}{\chi}\{\mathbf{M}^C \cdot \mathbf{N}^L(\chi[1-q]) + \mathbf{M}^L \cdot \mathbf{N}^L(\chi)\} = -2\mathbf{N}^{(2)}(\chi), \tag{C2}$$

and the next-to-leading order is determined by

$$\int_0^1 \frac{\mathrm{d}q}{\chi}\{\mathbf{M}^C \cdot \mathbf{N}^{NL}(\chi[1-q]) + \mathbf{M}^L \cdot \mathbf{N}^{NL}(\chi)\} = \mathbf{N}^L(\chi). \tag{C3}$$

We solve these equations by expanding in χ,

$$\mathbf{N}^{L,NL} = \left\{\sum_{m=0}^{m_{\max}} A_m^{L,NL}\chi^m, \sum_{m=1}^{m_{\max}} B_m^{L,NL}\chi^m\right\} e^{-\frac{16}{3\chi}}, \tag{C4}$$

where A_m and B_m are constants to be determined. Performing the q integral in (C2), as explained in Appendix A, gives a χ expansion that we then match with (A9). We find

$$\{A_0^L, A_1^L, A_2^L, \ldots\} = \{0.0439398, 0.0839502, -0.157605, \ldots\} \tag{C5}$$

and

$$\{B_0^L, B_1^L, B_2^L, \ldots\} = \{-0.0242686, 0.0919387, -0.633781, \ldots\}. \tag{C6}$$

We have calculated terms up to $m_{\max} = 25$. Next, we solve (C3) in the same way and obtain A_m^{NL} and B_m^{NL}. These coefficients grow factorially with alternating sign. We can therefore once again use Borel-Padé to resum the χ expansions and obtain $\mathbf{N}^L(\chi)$ and $\mathbf{N}^{NL}(\chi)$. The resulting approximation (C1) agrees well with the large T limit of the exact result.

Equation (C1) obviously breaks down for small T, since $\mathbf{N} \approx T^2\mathbf{N}^{(2)}$ for $T \ll 1$. However, we can, without doing any extra calculations, significantly improve this approximation by simply making the replacement $aT + b \to F(T,+1), F(T,-1)$ or $(F(T,+1) + F(T,-1))/2$, where

$$F(T,\epsilon) = aT + b + \left(\epsilon\sqrt{a^2+2bc}\,T - b\right)\exp\left(\frac{a+\epsilon\sqrt{a^2+2bc}}{b}T\right). \tag{C7}$$

In cases where the square root is complex, $(F(T,+1) + F(T,-1))/2$ is real. The exponential term does not affect the results at large T since it is exponentially suppressed compared to $aT + b$. But for $T \ll 1$, we have, thanks to the added exponential,

$$F(T) \approx cT^2, \tag{C8}$$

so by choosing $\mathbf{c}$ such that $\mathbf{N}^{(\mathrm{approx})} \approx T^2\mathbf{N}^{(2)}$, we have an approximation that is correct at both $T \gg 1$ and $T \ll 1$. Since $\mathbf{N}$ has a rather simple behavior, one can expect that $\mathbf{N}^{(\mathrm{approx})}$ will not be far from $\mathbf{N}$ even at intermediate values of T. The results are shown in Figs. 2–4. We can see that in all cases, using (C7) indeed gives an improvement. From Fig. 3, we see that for $\chi = 0.3$, the improvement (C7) gives a good precision even at intermediate values of T where $(P_\downarrow - P_\uparrow)/2$ changes sign. However, from Fig. 4, we see that for $\chi = 5$, the improvement (C7) only gives a qualitative agreement at intermediate values of T. But this is not surprising since we should not expect to always be able to obtain a precise approximation using only the leading order in $T \ll 1$ and the leading and next-to-leading orders in $T \gg 1$. Since one anyway needs to include other diagrams (fermion loops) and processes to obtain physical results at such large values of χ, and since we anyway can obtain good precision up to large T by resumming only the $T \ll 1$ expansion coefficients, we leave it to future studies to find ways to obtain higher orders in $T \gg 1$ or to combine the leading and next-to-leading order in $T \gg 1$ with more terms from the $T \ll 1$ expansion.

APPENDIX D: CIRCULARLY POLARIZED MONOCHROMATIC FIELD

To illustrate our methods, we have used as examples a constant field and a Sauter pulse, both linearly polarized. We have seen that they both predict a similar change of sign for $P_\uparrow - P_\downarrow$ at $T < 1$ but lead to very different behavior at $T \gg 1$. Note that we have treated both fields with a locally-constant-field (LCF) approach, so that is not the reason for

the difference. The reason is rather the shape of the field: a Sauter pulse versus a flat top. As the constant field might seem less relevant from an experimental point of view, one may therefore wonder how relevant that example is for large T, beyond illustrating the mathematics. Here, we will show that one can expect similar behavior for a circularly polarized monochromatic field, which we expect to be a good first approximation for a circularly polarized field with a long, essentially flat envelope. As long as the field is sufficiently long (contains enough oscillations), we do not have to assume that a_0 is large, because the incoherent products of first-order Mueller matrices give the dominant contribution for either large a_0 or a long pulse. However, the Mueller matrices that we have focused on so far in this paper have been the ones for the LCF regime, which work for large a_0. Now, we will instead use the monochromatic-field approximations[11] of the Mueller matrices [38]. In the LCF case, the Mueller matrices are expressed in terms of Airy functions. Here, the most nontrivial parts can instead be expressed in terms of three integrals, $\mathcal{J}_0$, $\mathcal{J}_1$, and $\mathcal{J}_2$, which are given in Appendix A in Ref. [38]. Although they can be expressed as sums of products of Bessel functions, for our present purposes, it is more convenient to use their integral representations. For $\mathcal{J}_0$, we have

$$\mathcal{J}_0 = \frac{i}{2\pi}\int \frac{\mathrm{d}\theta}{\theta}\exp\left\{\frac{ir}{2b_0}\Theta\right\}, \tag{D1}$$

where the integration contour is one that is equivalent to replacing $\theta \to \theta + i\epsilon$ ($\epsilon > 0$) and then integrating along the real axis, r and b_0 denote the same quantities as in the LCF case (e.g., for the pair-production step, we have $r = (1/s_2) + (1/s_3)$ and $b_0 = kl$), and the "effective mass" (M^2) part is given in this approximation by

$$\Theta = \theta M^2 = \theta\left[1 + a_0^2\left(1 - \mathrm{sinc}^2\frac{\theta}{2}\right)\right]. \tag{D2}$$

The integrands for $\mathcal{J}_1$ and $\mathcal{J}_2$ have the same exponential but different preexponentials; see Eqs. (A2) and (A3) in Ref. [38]. These representations are convenient because in the low-energy limit, $b_0 \ll 1$, we can perform the integrals using the saddle-point approximation. The saddle-point equation

$$\frac{\mathrm{d}\Theta}{\mathrm{d}\theta} = 0 \tag{D3}$$

cannot be solved analytically but is trivial so solve numerically. In the LCF case, $a_0 \gg 1$, we would rescale $\theta \to \hat{\theta}/a_0$

[11]We could use them to treat the field as locally monochromatic, but here we will for simplicity consider a constant, flat envelope.

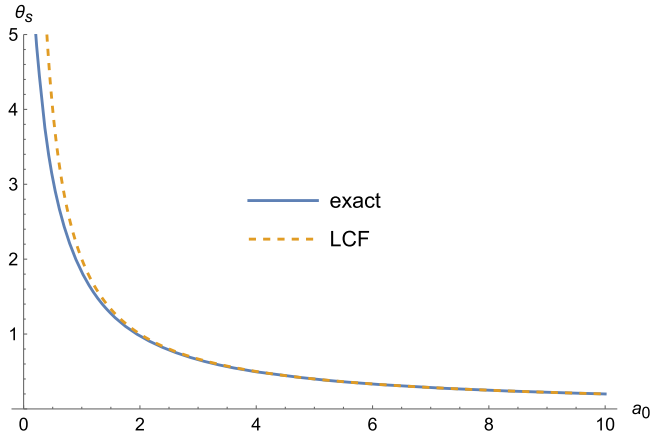

FIG. 7. The saddle point for the θ integral in (D1).

and expand the integrand in $1/a_0 \ll 1$ with $\chi = a_0 b_0$ kept constant. For the exponent, this gives

$$a_0\Theta \to \hat{\theta}\left(1 + \frac{\hat{\theta}^2}{12}\right), \tag{D4}$$

which has a saddle point at $\hat{\theta} = 2i$ (and another one at $-2i$, which does not contribute). So, for large a_0, the solution to (D3) should approach $2i/a_0$. As shown in Fig. 7, the convergence is quite fast.

Just as in the LCF case, here, too, the Stokes vectors only have two relevant components. However, the special spin/polarization states are different. In the LCF case, $\mathbf{N}_\gamma = \{1, \pm 1\}$ correspond to photon polarization parallel to the electric and magnetic field components, and for fermions, $\mathbf{N} = \{1, \pm 1\}$ correspond to spin parallel or antiparallel to the magnetic field. Here, $\mathbf{N}_\gamma = \{1, \pm 1\}$ instead corresponds to circular polarization, and $\mathbf{N} = \{1, \pm 1\}$ corresponds to spin along the laser propagation direction.

We start again with the latest vertex. By summing over the spin of the final-state particles, we find in general that we do not need to consider photon emissions and the fermion-mass loops on the fermion lines after vertex A and B in Fig. 1. So, the last vertex is again B. We again need a Mueller vector rather than a Mueller matrix, which takes into account the polarization of the intermediate photon. The relevant expressions can be found in Eqs. (31), (32), and (35) in Ref. [38]. We have two integrals to perform, over θ and the longitudinal momentum of the positron, s_3. We perform both with the saddle-point method. We have a saddle point at $s_3 = 1/2$, where the positron and electron share the momentum equally.

Consider the fermion loops between vertex A and B in Fig. 1. They can be resummed as in Eq. (161) in Ref. [38]. To leading exponential order (i.e., neglecting production of more than one pair), only the terms that lead to a rotation of the photon Stokes vector (i.e., vacuum birefringence) remain, but a Stokes vector for a purely circularly polarized

photon is not affected. So, these loops do not contribute here, and hence the next step after B is A. For this, we need the parts of the Mueller matrix for Compton scattering which take into account the polarization of the emitted photon and the spin of the electron before emission. The relevant expressions are given by Eqs. (22), (23), (26), and (28) in Ref. [38]. We again have two integrals. The θ integral is the same as for the B vertex. The integral over the longitudinal momentum of the emitted photon has a saddle point at $q = 2/3$, which means all three final-state fermions have the same longitudinal momentum ($1 = s_1 + s_2 + s_3 = 3s_1$, so $q = 1 - s_1 = 2/3$).

For the photon emission and loops up to vertex C, we find a similar recursive formula as in (10),

$$\mathbf{N}^{(n)} = \int_0^1 \frac{\mathrm{d}q}{nb_0}\{\mathbf{M}^C \cdot \mathbf{N}^{(n-1)}([1-q]b_0) + \mathbf{M}^L \cdot \mathbf{N}^{(n-1)}(b_0)\}. \tag{D5}$$

In this case, we use $T = \Delta\sigma\alpha$ without a factor of a_0. In the limit of large a_0, it would again be natural to use $T = \Delta\sigma a_0\alpha$ instead, but that is not a natural expansion parameter for $a_0 < 1$, and here we can consider both large and small[12] a_0. Here, we consider for simplicity only $\langle P\rangle$ and the leading order in $b_0 \ll 1$, so we only need the parts of $\mathbf{M}^C$ and $\mathbf{M}^L$ that describe unpolarized particles.[13] For $\mathbf{M}^C$, this is given by Eq. (23) in Ref. [38], and for $\mathbf{M}^L$, we have the same but with opposite sign. Similar to (12), we have

$$\{1,0\} \cdot \mathbf{N}^{(n)} = a_n \exp\left(-\frac{\mathcal{A}(a_0)}{b_0}\right), \tag{D6}$$

but with different a_n of course. In these steps, the θ and q integrals cannot be performed with the saddle-point method. We can, though, still calculate the q integral analytically, e.g., by changing variable from q to $\gamma = r/b_0$, where $r = (1/s_1) - 1$ (same as before) and then expanding to leading order in $b_0 \ll 1$. Then, we see that the dominant contribution in theses steps comes from soft photons, $q = \mathcal{O}(b_0)$, in contrast to vertex A where the photon takes $2/3$ of the electron momentum. The recursive formula simplifies to

$$a_n = -\frac{d_c}{n} a_{n-1}, \tag{D7}$$

which is the same equation as for the LCF case (A25), except that the starting point a_2 and the coefficient d_c are now nontrivial functions of a_0. We find

[12]The incoherent-product approximation breaks down in the limit where a_0 becomes small and $\Delta\sigma$ is fixed, but if we compensate by making $\Delta\sigma$ larger, then we can consider small a_0.

[13]Note, though, that we still have to take the polarization of the intermediate photon into account, even if we only consider an unpolarized initial electron.

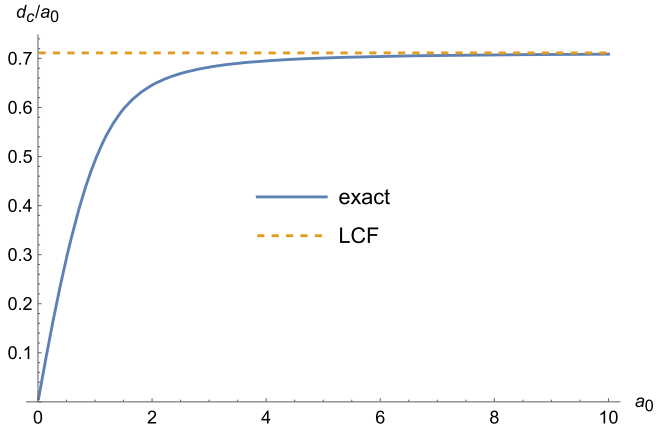

FIG. 8. d as in (D8) and the LCF result (A26).

$$\begin{aligned} d_c(a_0) &= -\frac{i}{2\pi}\int \frac{\mathrm{d}\theta}{\theta}\left(1 + 2a_0^2\sin^2\frac{\theta}{2}\right) \\ &\quad \times \int_0^\infty \mathrm{d}\gamma(1 - e^{-\mathcal{A}\gamma})\exp\left(\frac{i\Theta\gamma}{2}\right) \\ &= \frac{1}{\pi}\int \frac{\mathrm{d}\theta}{\theta}\left(1 + 2a_0^2\sin^2\frac{\theta}{2}\right)\left(\frac{1}{\Theta} - \frac{1}{\Theta + 2i\mathcal{A}}\right). \end{aligned} \tag{D8}$$

The remaining θ integral has a complicated dependence on a_0 and cannot be approximated unless we consider $a_0 \gg 1$

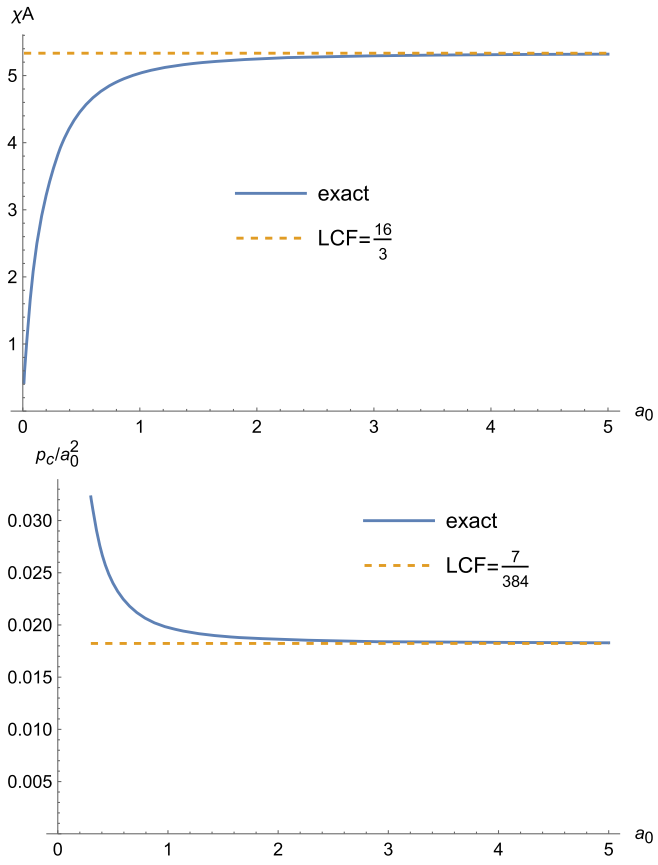

FIG. 9. The exponent and prefactor in (D9).

or $a_0 \ll 1$, but it can be performed numerically, e.g., with a contour parallel and just above the real axis. Thus, in the low-energy limit, we find

$$\langle P \rangle = p_c(a_0) T^2 F[d_c(a_0) T] \exp\left(-\frac{\mathcal{A}(a_0)}{b_0}\right), \tag{D9}$$

where F is the same function as in (17) for the LCF case. d_c and $\mathcal{A}$ are plotted in Figs. 8 and 9, which show that for large a_0 we recover the LCF results.

The $a_0 \gg 1$ limit of $p_c(a_0)$ in (D9) also agrees with what one can expect from an LCF approach. However, this is not simply the factor of $1/2 \times 32$ in (15). To get the correct LCF approximation, we need to take into account the fact that the field rotates and therefore does not in general point in the same direction in vertex A and B in Fig. 1. To obtain the LCF version of p_c, it is enough to consider $\mathcal{O}(\alpha^2)$, which is given by Eq. (65) in Ref. [38]. What is important to emphasize here is that there are two σ integrals, σ_1 and σ_2 for vertex A and B, and the integrand has two terms: one is the product of the average "rates," and the second is related to the polarization of the intermediate photon. The second term oscillates as $\cos[2(\sigma_2 - \sigma_1)]$ for a circularly polarized field and therefore averages out for a long pulse, while for a constant field with linear polarization, it is on the same order of magnitude as the first term. In the low-energy limit that we consider here we can perform the θ and longitudinal momentum integrals with the saddle-point method. For the constant field, we find

$$\{1, 0\} \cdot \mathbf{N}^{(2)} = \frac{1}{384}(7 - 1) = \frac{1}{2 \times 32}, \tag{D10}$$

while for a circularly polarized field, we have just the first term

$$\{1, 0\} \cdot \mathbf{N}^{(2)} = \frac{7}{384}. \tag{D11}$$

In Fig. 9, we see that, by taking this into account, we find agreement also for p_c in the LCF limit.

We plan to consider the spin dependence in detail elsewhere, e.g., $P_\uparrow - P_\downarrow$. Here, we just note that, for a circular field, it is natural to consider $\Delta P(\|\mathbf{k}) = P_{\uparrow\mathbf{k}} - P_{\downarrow\mathbf{k}}$ for an initial electron that has spin up or down the laser propagation direction ($\mathbf{k}$). There is no limit where one should expect this to be equal to (16), which corresponds to spin up or down the magnetic field direction, $\Delta P(\|\mathbf{B}) = P_{\uparrow\mathbf{B}} - P_{\downarrow\mathbf{B}}$; i.e., $\Delta P(\|\mathbf{k})$ and $\Delta P(\|\mathbf{B})$ are simply two different quantities. $\Delta P(\|\mathbf{B})$ in a monochromatic field just averages to zero, while $\Delta P(\|\mathbf{k})$ is negligible compared to $\langle P \rangle$ for large a_0.

[1] C. Bamber, S. J. Boege, T. Koffas, T. Kotseroglou, A. C. Melissinos, D. D. Meyerhofer, D. A. Reis, W. Ragg, C. Bula, K. T. McDonald *et al.*, Studies of nonlinear QED in collisions of 46.6-GeV electrons with intense laser pulses, Phys. Rev. D **60**, 092004 (1999).

[2] V. N. Baier, V. M. Katkov, and V. M. Strakhovenko, Higher-order effects in external field: Pair production by a particle, Sov. J. Nucl. Phys. **14**, 572 (1972).

[3] V. I. Ritus, Vacuum polarization correction to elastic electron and muon scattering in an intense field and pair electro- and muoproduction, Nucl. Phys. **B44**, 236 (1972).

[4] H. Hu, C. Muller, and C. H. Keitel, Complete QED Theory of Multiphoton Trident Pair Production in Strong Laser Fields, Phys. Rev. Lett. **105**, 080401 (2010).

[5] A. Ilderton, Trident Pair Production in Strong Laser Pulses, Phys. Rev. Lett. **106**, 020404 (2011).

[6] B. King and H. Ruhl, Trident pair production in a constant crossed field, Phys. Rev. D **88**, 013005 (2013).

[7] H. Hu and J. Huang, Trident pair production in colliding bright x-ray laser beams, Phys. Rev. A **89**, 033411 (2014).

[8] K. Krajewska and J. Z. Kamiński, Circular dichroism in nonlinear electron-positron pair creation, J. Phys. Conf. Ser. **594**, 012024 (2015).

[9] V. Dinu and G. Torgrimsson, Trident pair production in plane waves: Coherence, exchange, and spacetime inhomogeneity, Phys. Rev. D **97**, 036021 (2018).

[10] B. King and A. M. Fedotov, Effect of interference on the trident process in a constant crossed field, Phys. Rev. D **98**, 016005 (2018).

[11] F. Mackenroth and A. Di Piazza, Nonlinear trident pair production in an arbitrary plane wave: A focus on the properties of the transition amplitude, Phys. Rev. D **98**, 116002 (2018).

[12] U. Hernandez Acosta and B. Kämpfer, Laser pulse-length effects in trident pair production, Plasma Phys. Controlled Fusion **61**, 084011 (2019).

[13] V. Dinu and G. Torgrimsson, Trident process in laser pulses, Phys. Rev. D **101**, 056017 (2020).

[14] G. Torgrimsson, Nonlinear trident in the high-energy limit: Nonlocality, Coulomb field and resummations, Phys. Rev. D **102**, 096008 (2020).

[15] A. Di Piazza, C. Muller, K. Z. Hatsagortsyan, and C. H. Keitel, Extremely high-intensity laser interactions with fundamental quantum systems, Rev. Mod. Phys. **84**, 1177 (2012).

[16] A. Gonoskov, T. G. Blackburn, M. Marklund, and S. S. Bulanov, Charged particle motion and radiation in strong electromagnetic fields, Rev. Mod. Phys. **94**, 045001 (2022).

[17] A. Fedotov, A. Ilderton, F. Karbstein, B. King, D. Seipt, H. Taya, and G. Torgrimsson, Advances in QED with intense background fields, arXiv:2203.00019.

[18] H. Abramowicz, U. Acosta, M. Altarelli, R. Aßmann, Z. Bai, T. Behnke, Y. Benhammou, T. Blackburn, S. Boogert, and O. Borysov *et al.*, Conceptual design report for the LUXE experiment, Eur. Phys. J. Special Topics **230**, 2445 (2021).

[19] S. Meuren, P. H. Bucksbaum, N. J. Fisch, F. Fiúza, S. Glenzer, M. J. Hogan, K. Qu, D. A. Reis, G. White, and V. Yakimenko, On seminal HEDP research opportunities enabled by colocating multi-petawatt laser with high-density electron beams, arXiv:2002.10051.

[20] T. Heinzl, A. Ilderton, and B. King, Classical Resummation and Breakdown of Strong-Field QED, Phys. Rev. Lett. **127**, 061601 (2021).

[21] G. Torgrimsson, Resummation of Quantum Radiation Reaction in Plane Waves, Phys. Rev. Lett. **127**, 111602 (2021).

[22] G. Torgrimsson, Resummation of quantum radiation reaction and induced polarization, Phys. Rev. D **104**, 056016 (2021).

[23] R. Ekman, T. Heinzl, and A. Ilderton, Reduction of order, resummation, and radiation reaction, Phys. Rev. D **104**, 036002 (2021).

[24] R. Ekman, Reduction of order and transseries structure of radiation reaction, Phys. Rev. D **105**, 056016 (2022).

[25] F. Karbstein, All-Loop Result for the Strong Magnetic Field Limit of the Heisenberg-Euler Effective Lagrangian, Phys. Rev. Lett. **122**, 211602 (2019).

[26] F. Karbstein, Large N external-field quantum electrodynamics, J. High Energy Phys. 01 (2022) 057.

[27] A. A. Mironov, S. Meuren, and A. M. Fedotov, Resummation of QED radiative corrections in a strong constant crossed field, Phys. Rev. D **102**, 053005 (2020).

[28] A. A. Mironov and A. M. Fedotov, Structure of radiative corrections in a strong constant crossed field, Phys. Rev. D **105**, 033005 (2022).

[29] J. P. Edwards and A. Ilderton, Resummation of background-collinear corrections in strong field QED, Phys. Rev. D **103**, 016004 (2021).

[30] T. Podszus and A. Di Piazza, First-order strong-field QED processes including the damping of particle states, Phys. Rev. D **104**, 016014 (2021).

[31] T. Podszus, V. Dinu, and A. Di Piazza, Nonlinear Compton scattering and nonlinear Breit-Wheeler pair production including the damping of particle states, Phys. Rev. D **106**, 056014 (2022).

[32] V. I. Ritus, Radiative corrections in quantum electrodynamics with intense field and their analytical properties, Ann. Phys. (N.Y.) **69**, 555 (1972).

[33] N. B. Narozhnyi, Expansion parameter of perturbation theory in intense field quantum electrodynamics, Phys. Rev. D **21**, 1176 (1980).

[34] H. Gies and F. Karbstein, An Addendum to the Heisenberg-Euler effective action beyond one loop, J. High Energy Phys. 03 (2017) 108.

[35] N. Ahmadiniaz, J. P. Edwards, and A. Ilderton, Reducible contributions to quantum electrodynamics in external fields, J. High Energy Phys. 05 (2019) 038.

[36] A. Di Piazza and F. P. Fronimos, Quasiclassical representation of the Volkov propagator and the tadpole diagram in a plane wave, Phys. Rev. D **105**, 116019 (2022).

[37] S. Meuren and A. Di Piazza, Quantum Electron Self-Interaction in a Strong Laser Field, Phys. Rev. Lett. **107**, 260401 (2011).

[38] G. Torgrimsson, Loops and polarization in strong-field QED, New J. Phys. **23**, 065001 (2021).

[39] V. Dinu and G. Torgrimsson, Approximating higher-order nonlinear QED processes with first-order building blocks, Phys. Rev. D **102**, 016018 (2020).

[40] S. Bragin, S. Meuren, C. H. Keitel, and A. Di Piazza, High-Energy Vacuum Birefringence and Dichroism in an Ultrastrong Laser Field, Phys. Rev. Lett. **119**, 250403 (2017).

[41] B. King and N. Elkina, Vacuum birefringence in high-energy laser-electron collisions, Phys. Rev. A **94**, 062102 (2016).

[42] M. Tamburini and S. Meuren, Efficient high-energy photon production in the supercritical QED regime, Phys. Rev. D **104**, L091903 (2021).

[43] I. V. Sokolov, N. M. Naumova, J. A. Nees, and G. A. Mourou, Pair Creation in QED-Strong Pulsed Laser Fields Interacting with Electron Beams, Phys. Rev. Lett. **105**, 195005 (2010).

[44] N. V. Elkina, A. M. Fedotov, I. Y. Kostyukov, M. V. Legkov, N. B. Narozhny, E. N. Nerush, and H. Ruhl, QED cascades induced by circularly polarized laser fields, Phys. Rev. ST Accel. Beams **14**, 054401 (2011).

[45] N. Neitz and A. Di Piazza, Electron-beam dynamics in a strong laser field including quantum radiation reaction, Phys. Rev. A **90**, 022102 (2014).

[46] D. Seipt, C. P. Ridgers, D. Del Sorbo, and A. G. R. Thomas, Polarized QED cascades, New J. Phys. **23**, 053025 (2021).

[47] R. A. Askey and R. Roy, Gamma Function, NIST Digital Library of Mathematical Functions, https://dlmf.nist.gov/5.9.

[48] D. Seipt, D. Del Sorbo, C. P. Ridgers, and A. G. R. Thomas, Ultrafast polarization of an electron beam in an intense bichromatic laser field, Phys. Rev. A **100**, 061402 (2019).

[49] Y. Y. Chen, P. L. He, R. Shaisultanov, K. Z. Hatsagortsyan, and C. H. Keitel, Polarized Positron Beams via Intense Two-Color Laser Pulses, Phys. Rev. Lett. **123**, 174801 (2019).

[50] H. H. Song, W. M. Wang, and Y. T. Li, Generation of polarized positron beams via collisions of ultrarelativistic electron beams, Phys. Rev. Res. **3**, 033245 (2021).

[51] T. G. Blackburn, A. Ilderton, C. D. Murphy, and M. Marklund, Scaling laws for positron production in laser–electron-beam collisions, Phys. Rev. A **96**, 022128 (2017).

[52] A. Di Piazza, Exact solution of the Landau-Lifshitz equation in a plane wave, Lett. Math. Phys. **83**, 305 (2008).

[53] H. Heintzmann and M. Grewing, Acceleration of charged particles and radiation-reaction in strong plane and spherical waves, Z. Phys. **251**, 77 (1972).

[54] Y. F. Li, Y. Y. Chen, W. M. Wang, and H. S. Hu, Production of Highly Polarized Positron Beams via Helicity Transfer from Polarized Electrons in a Strong Laser Field, Phys. Rev. Lett. **125**, 044802 (2020).

[55] V. I. Ritus, Quantum effects of the interaction of elementary particles with an intense electromagnetic field, J. Russ. Laser Res. **6**, 497 (1985).

[56] H. R. Reiss, Absorption of light by light, J. Math. Phys. (N.Y.) **3**, 59 (1962).
[57] A. I. Nikishov and V. I. Ritus, Quantum processes in the field of a plane electromagnetic wave and in a constant field 1, J. Exp. Theor. Phys. **19**, 529 (1964).
[58] G. Degli Esposti and G. Torgrimsson, Worldline instantons for nonlinear Breit-Wheeler pair production and Compton scattering, Phys. Rev. D **105**, 096036 (2022).
[59] O. Costin and G. V. Dunne, Resurgent extrapolation: Rebuilding a function from asymptotic data. Painlevé I, J. Phys. A **52**, 445205 (2019).
[60] O. Costin and G. V. Dunne, Physical resurgent extrapolation, Phys. Lett. B **808**, 135627 (2020).
[61] E. Caliceti, M. Meyer-Hermann, P. Ribeca, A. Surzhykov, and U. Jentschura, From useful algorithms for slowly convergent series to physical predictions based on divergent perturbative expansions, Phys. Rep. **446**, 1 (2007).
[62] A. Florio, Schwinger pair production from Padé-Borel reconstruction, Phys. Rev. D **101**, 013007 (2020).
[63] G. V. Dunne and Z. Harris, On the higher loop Euler-Heisenberg trans-series structure, Phys. Rev. D **103**, 065015 (2021).
[64] G. A. Baker, Application of the padé approximant method to the investigation of some magnetic properties of the Ising model, Phys. Rev. **124**, 768 (1961).
[65] C. M. Bender and S. A. Orszag, *Advanced Mathematical Methods for Scientists and Engineers, Asymptotic Methods and Perturbation Theory* (Springer-Verlag, New York 1999).
[66] H. Kleinert and V. Schulte-Frohlinde, *Critical Properties of ϕ^4-Theories* (World Scientific, Singapore, 2001).
[67] J. Zinn-Justin, *Quantum Field Theory and Critical Phenomena*, 4th ed. (Clarendon Press, Oxford, 2002).
[68] J. C. Le Guillou and J. Zinn-Justin, Critical exponents from field theory, Phys. Rev. B **21**, 3976 (1980).
[69] H. Mera, T. G. Pedersen, and B. K. Nikolić, Fast summation of divergent series and resurgent transseries from Meijer- G approximants, Phys. Rev. D **97**, 105027 (2018).
[70] G. Álvarez and H. J. Silverstone, A new method to sum divergent power series: Educated match, J. Phys. Commun. **1**, 025005 (2017).
[71] G. Torgrimsson, Nonlinear photon trident versus double Compton scattering and resummation of one-step terms, Phys. Rev. D **102**, 116008 (2020).